http://www.aimspress.com/journal/Materials

Research article

Influence of laser marking parameters on data matrix code quality on polybutylene terephthalate/glass fiber composite surface using microscopy and spectroscopy techniques

R.C.M. Sales-Contini[1,2,*], J.P. Costa[1], F.J.G. Silva[1,3,5], A.G. Pinto[1], R.D.S.G. Campilho[1,3,5], I.M. Pinto[1,4], V.F.C. Sousa[1,3] and R.P. Martinho[1]

[1] ISEP, Polytechnic of Porto, Rua Dr. António Bernardino de Almeida, 4249-015 Porto, Portugal
[2] College of Technology São José dos Campos, Professor Jessen Vidal, Centro Paula Souza, Avenida Cesare Mansueto Giulio Lattes, 1350 Distrito Eugênio de Melo, 12247-014, São José dos Campos/SP, Brazil
[3] INEGI - Institute of Science and Innovation in Mechanical Engineering and Industrial Engineering, Porto, Portugal
[4] Mathematical Engineering Laboratory, LEMA, Porto, Portugal
[5] Associate Laboratory for Energy, Transports and Aerospace (LAETA-INEGI), Rua Dr. Roberto Frias 400, 4200-465 Porto, Portugal

* Correspondence: Email: rcmsc@isep.ipp.pt; Tel: +351-934-983-427.

Abstract: Laser marking on polymer composite surfaces can be difficult to read and cause readability problems for electronic decoding equipment on production lines due to poor interaction between the laser and the fibers used to reinforce these materials. This problem can be solved with the right choice of marking parameters, resulting in savings for companies by avoiding production problems such as rejection, scrap and customer complaints. The present work uses the polybutylene terephthalate/glass fiber (PBT/GF) composite used in the manufacture of instrument panels for motorcycles. The tests were carried out with different laser marking parameters using a neodymium:yttrium-aluminum-garnet (Nd:YAG) laser. Subsequently, the laser-marked data matrix codes (DMC) were analyzed using a microscope verifier to evaluate the quality according to the ISO/IEC 29158:2020 standard. A detailed analysis of these surfaces was also carried out to observe some physical and chemical changes using scanning electron microscopy (SEM) and energy dispersive X-ray spectroscopy (EDS). The optical analysis showed that lower radiation power and pulse frequency and higher marking speed corresponded to weaker laser

marking and therefore poorer DMC code quality, which was confirmed by the SEM. EDS showed that the laser marking process did not cause the chemical changes on the sample surface.

1. Introduction

As a result of global industrial competitiveness, companies are increasingly investing in technology and digitalization to improve operational efficiency, productivity, quality, production times and other outcomes in their production processes, to guarantee the quality of the final products and reduce production costs [1,2]. The new industrial revolution, Industry 4.0, brings increasing automation and digitization through the Internet of Things (IoT) [3]. These codes are defined as a 2D barcode used to store a large amount of data in a grid of black and white squares that can be placed in either a square or rectangular form. They can be directly marked with a laser on the material surface, providing permanent, legible marking and effective traceability, but the quality of the printed code can be affected by the material, process parameters and type of laser used in the marking process [4–6].

Laser engraving is the most widely used technique to produce a high-quality marked surface, marking the material by creating grooves. It can be used on both metallic and polymeric materials. The penetration depth can be a few millimeters, depending on the number of passes made. This method requires the energy density to be high enough to raise the surface temperature of the material well above the melting point, causing melting or evaporation [7–9].

Laser interactions in metal materials were studied by Qi et al. [10]. They investigated the influence of pulse frequency on the marking quality of stainless steel by analyzing the width, depth (penetration) and contrast using scanning electron microscopy (SEM), energy dispersive X-ray spectroscopy (EDS), a profilometer, and a special imaging device. It was observed that the presence of oxygen in the markings was higher at higher values of pulse frequency due to increased oxidation of the material. They concluded that the pulse frequency has a significant effect on the quality of the marking, as an increase in the pulse frequency results in less evaporation of the material and more oxidation, which increases the contrast [10].

Jangsombatsiri and Porter [11] established a relationship between laser marking parameters and the quality obtained in data matrix codes (DMC) marked on cold rolled carbon steel substrates AISI C1008/1010 and AISI C1095. The parameters were tested using factorial experiment planning. The qualities of all DMC were assessed according to ISO/IEC 16022:2006. The authors used SEM to check the conditions of the substrates before and after marking and EDS to determine the chemical compositions of the substrate surfaces after marking. It was concluded that the laser parameters should be carefully selected to avoid residues that may generate an unacceptable final quality grade. The pulse frequency and the radiation power directly influenced the quality obtained in the marked DMC.

In addition to metallic materials, composite materials, polymeric materials and their nanocomposites have been increasingly used in the manufacture of aerospace and automotive parts due to their low weight, high modulus, chemical resistance, and excellent wear resistance [12]. Within the production process, parts made from polymer materials must also be easily traceable to ensure the quality of the final product. Since laser marking is fast and effective for most materials used in production, it is necessary to understand the influence of laser parameters on the surfaces of these materials.

The nature of the laser-material interaction and the quality of the laser marking are highly dependent on both the material composition and the laser settings. Some polymers receive additives to facilitate laser marking and improve the quality of the codes; these include polypropylene (PP) [13], acrylonitrile butadiene styrene (ABS) [14,15], and polyamide (PA) [16]. Some authors have studied the performance of laser marking on the surfaces of polymeric materials with the addition of nanocomposites. Changes in surface morphology and structure of composite materials were observed by Raman spectroscopy and scanning electron microscopy techniques after using the laser marking process [17].

Czyzewski et al. [13] studied laser marking on the surface of polypropylene with laser-marking additives (PP-LMA). They observed that a low value of radiation power can influence the quality of marked codes. It was also observed by SEM that a high additive percentage promotes a higher production of laser beam spots on the mold surface than samples with lower additive content. They also observed that higher frequency and speed can influence the space between the dots. These irregularities can affect code quality.

Cheng et al. [18] studied the carbonization mechanism of the laser marking process on polypropylene/antimony-doped tin oxide@polyimide (PP/ATO@PI) and polypropylene/antimony-doped tin oxide (PP/ATO) composite surfaces. Using SEM, transmission electron microscopy (TEM), Raman spectroscopy, and near-infrared (NIR) spectroscopy, they observed, after irradiation from a 1064 nm laser, that the PP/ATO@PI composite promoting the best black laser-induced pattern comes from the local carbonization of the polymer surface subject to the laser irradiation and a more efficient and environmentally friendly process.

Other polymers, such as polycarbonate (PC) [19], polystyrene (PS) [12], thermoplastic polyurethane (TPU) [20,21], and polyethylene terephthalate (PET) and polybutylene terephthalate (PBT) [22,23] are susceptible to laser light at this wavelength and produce carbonized dark marks on their surfaces. The marking mechanism is the combination of blackening by carbonization and brightening by microbubbles. Normally, plastic materials are marked with a neodymium:yttrium-aluminum-garnet (Nd:YAG) laser at a wavelength of 1064 nm [16].

Zhong et al. [20] observed that the loading amount of Bi_2O_3 (bismuth oxide) added to TPU determined the marking contrast properties of the TPU/Bi_2O_3 composite materials. Bi_2O_3 dispersed in TPU absorbed the laser energy and heated the surrounding TPU matrix, leading to pyrolysis and carbonization of the TPU chains. Using optical microscope images, SEM, X-ray photoelectron spectroscopy (XPS), Raman spectroscopy, thermogravimetric analysis (TGA), and X-ray diffraction (XRD), they demonstrated that the Bi_2O_3 in the TPU can be partially reduced to black bismuth metal by carbonized materials, resulting in the marking contrast and visual appearance of the surface of the TPU/Bi_2O_3 composites.

In other studies, Cao et al. [21] observed that TPU/BiOCl (bismuth oxychloride) composite samples showed high-contrast black markings on the surface after laser treatment, depending on the BiOCl loading and laser pulse frequency, in terms of visual and microscopic analysis. Using XPS, XRD, and Raman spectroscopy, the results revealed that the laser-induced blackening on the composite surface entails laser absorption of the BiOCl particles and local heating of the surrounding TPU chains, leading to the generation of amorphous black carbonized materials and the reduction of BiOCl into black bismuth metal, contributing to the formation of the black-colored marking on composite surfaces.

PBT is a versatile polymer that can be injection molded and used to produce a variety of products using selective laser sintering (SLS) [24,25]. This polymer is relevant for industrial use, such as

automotive applications, due to its good mechanical properties, good thermal insulation, relatively low cost, and high production rates in geometrically complex parts. It can be used as a blend with a semi-crystalline or amorphous component, added as nanoparticles, or even combined with glass fiber to be used as a laser-welded joint composite [26].

Some studies have shown the influence on the PBT material surface promoted by laser marking using a Nd:YAG laser. Ng and Yeo [22,23] evaluated laser marking using a Nd:YAG laser on different materials' surfaces, such as metallic materials, stainless steel, and anodized aluminum, and compared the results with the polymeric materials, PBT and phenol-formaldehyde. In terms of maximum color difference values, anodized aluminum could be classified as low, with PBT and stainless steel as medium and phenol formaldehyde as high. In the next study [23], they analyzed the influence of the luminosity ratio based on spectral reflectance measurements on the material surface. It was observed that the optimum speed was highest for PBT and lowest for stainless steel. The markings on phenol-formaldehyde and anodized aluminum had the highest and lowest visibilities, respectively. In both studies, they concluded that the changes were related to the interaction of the laser with the material.

Ng and Yeo [27] investigated the use of spectrophotometers in the quantitative evaluation of four types of surfaces marked with a Nd:YAG laser. They found that in the polymeric materials, PBT and phenol formaldehyde, the spectra had discernible changes in the average reflectance obtained because of different marking speeds but that the reflectance trace of the spectrum of the metallic materials was not efficiently distinguished due to the nature of the material. Compared to metallic materials, the physical integrity of polymeric materials is more susceptible to temperature changes.

Few studies have shown the changes promoted by the laser marking parameters and their influence on the surfaces of polymeric composite materials analyzed by SEM. Therefore, the present work brings an outstanding contribution to this field. The main objective of the research is to analyze the surface aspects of an Ultradur B 4406 G6, PBT-GF30 FR (17) surface composed of PBT/30% GF modified by Nd:YAG lasers and the influence of laser marking parameters on the quality of the code produced. This material is widely produced by injection molding of the instrument panel back housing of motorcycles.

2. Materials and methods

2.1. Material

Figure 1 presents the exploded view of a typical motorcycle panel. This panel is composed of an instrumentation system that is enclosed in a back housing made of a thermoplastic composite produced by injection molding. The back housing material is composed of PBT/30% GF (Ultradur B 4406 G6, PBT-GF30 FR (17)) [28].
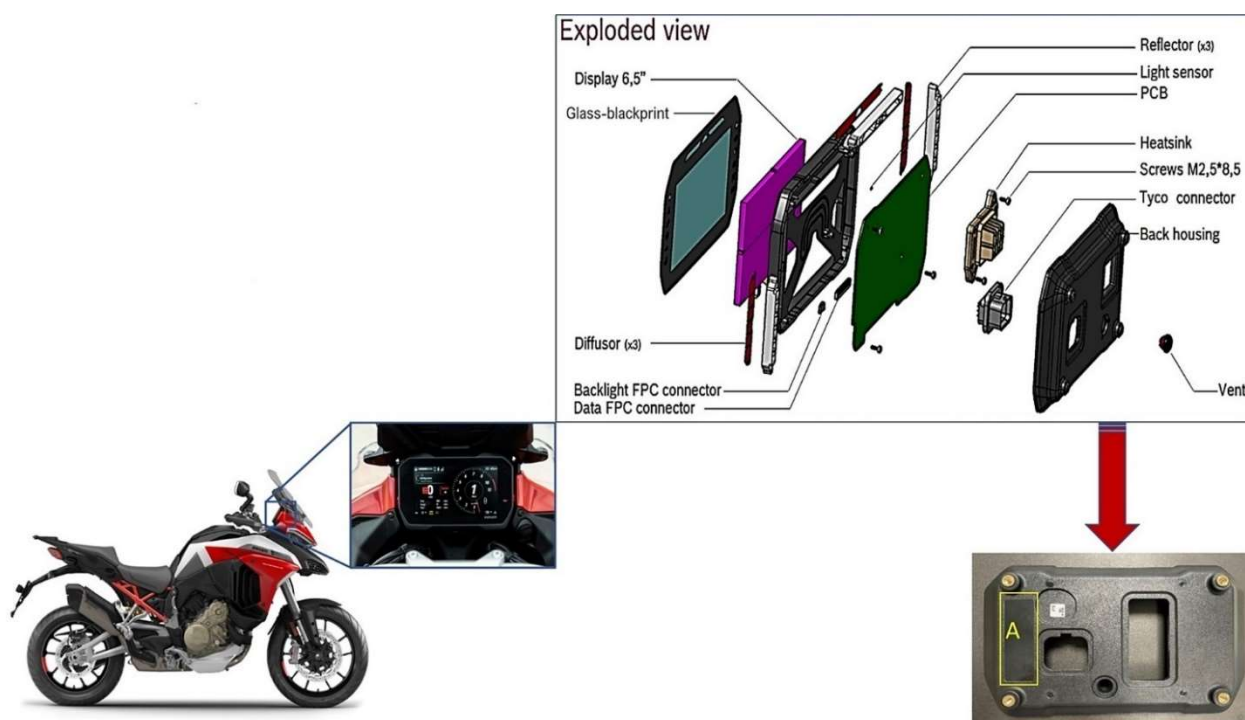
Figure 1. Exploded view of motorcycle instrument panel and back housing part. Region A: reserved area exclusively for the laser marking process.

2.2. Sample analyses and preparation before the laser marking process

Next, Rofin Coherent Visual Laser Marker (VLM) software was used to create the exclusive DMC that would be marked in the reserved area (region A in Figure 1). Once the marking software was created, the need for cleaning the lens, extraction system and surrounding area was determined. Cleaning was then carried out using tissue and methanol-based liquid. The focal length was adjusted so that the distance from the marking head reference to the workpiece surface was 432 mm.

After adjusting the focal length, a 9 × 9 mm code was marked on a part to be set up, and its size was confirmed using a Dino-Lite model AM3113T microscope, thus confirming the focal length. Next, a line was marked, and its thickness was measured with the same microscope, obtaining a value of 0.262 mm (Figure 2a). Using the value obtained, the thickness of the line was set in the VLM software.

The contour line function was activated when marking the modules to obtain codes with well-defined squares (Figure 2b). The dimensions of the modules were measured with the microscope used in the previous step, and the contour offset—the correction factor applied to the marking of the contour line—was adjusted using the VLM software until a uniform distribution was obtained between the size of the marked module and the space around it. For DMC, a correction of 0.06 mm was applied.
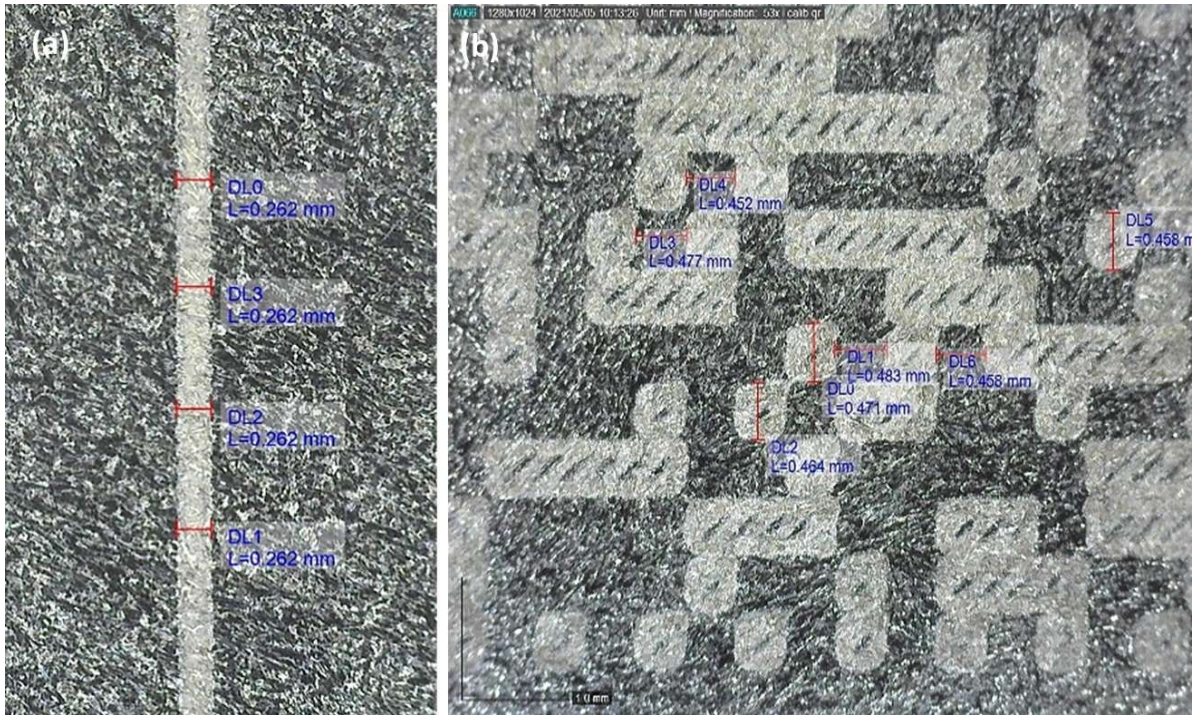
Figure 2. (a) Laser marking code line measurement and (b) laser marking code square measurement.

2.3. Laser marking equipment and parameters

For the laser marking process, Rofin + Coherent equipment was used. Inside this equipment, there is a fiber optic laser designated as the Power Line F20. The laser power is 20 W, with a wavelength of 1065 nm ± 5 nm produced by ytterbium (Yb) diodes. The laser system used a pulsed operating mode, spot diameter of 20 μm, pulse frequency (f) of 20–80 kHz, marking speed (V) of 0–20000 mm/s, pass-by overlap (S) of 0 to 100%, pulse length (τ) of 4–200 ns, working area of 120×120 mm^2, and temperature range of 15–35 °C.

As shown in Table 1, four laser marking parameters were considered in this work: radiation power (W), pulse frequency (kHz), marking speed (mm/s), and pass overlap (%).

Table 1. Laser marking parameters and their variations considered for the tests.

Factor	Name	Level	Level values		
A	Radiation power (W)	3	P_i	P_n	P_s
			15	17	19
B	Pulse frequency (kHz)	3	F_i	F_n	F_s
			15	25	30
C	Marking speed (mm/s)	3	V_i	V_n	V_s
			1000	2000	3000
D	Pass overlap (%)	3	S_i	S_n	S_s
			0	15	30

A complete factorial using design of experiments (DoE) was chosen considering the parameters recommended by the manufacturer, and the variations followed the following classifications: (i) higher value than recommended by the manufacturer, (ii) equal value as recommended by the manufacturer, and (iii) lower value than recommended by the manufacturer (BASF). The parameters for nominal radiation power, pulse frequency, marking speed, and pass overlap were 17 W, 25 kHz, 2000 mm/s, and 15%, respectively. The tests' parameters and the levels are established in Table 1.

The set of experiments to be performed was obtained with random parameter variation, in this case, 81 experiments; this result was obtained by increasing the number of levels to the number of factors 3^4 (3^4=4 factors with 3 levels each). The map of experiments performed and discussed in this work is shown in Table 2.

Table 2. Full-factorial DoE applied to the study to be carried out on the equipment.

Sample	Radiation power (W)	Pulse frequency (kHz)	Marking speed (mm/s)	Pass overlap (%)
I	15	25	2000	15
II	19	25	2000	15
III	17	30	2000	15
IV	17	25	3000	15
V	15	15	3000	0
VI	17	25	1000	15
VII	17	25	2000	15
VIII	19	30	1000	30
IX	17	15	2000	15

2.4. Quality assurance of laser-marked codes

Using an REA VeriCube Verifier, the laser-marked codes were accurately classified according to the characteristics of the codes. Each of the characteristics followed the criteria presented in ISO/IEC 29158:2020 [29], which can be A (4.0), B (3.0), C (2.0), D (1.0) or E (0.0), with A being the best and F being the worst. The overall quality class assigned to the code corresponds to the minimum classification of all these evaluated characteristics. All the marked codes, even those with a quality of F, could be decoded so that a positive decodability result was obtained for all the DMC. Once all the codes had been analyzed using the microscope Verifier, the results were exported to MS Excel, processed and correlated using Minitab software.

Regarding the response variables, the characteristics considered relevant to qualify the DMC were the following: (i) the ability of a code to be decoded by a decoding algorithm, such as a scanner = Decodability; (ii) the difference in reflectance value between the light and dark elements, and between the quiet zone and the peripheral elements = cell contrast (CC); (iii) reflection uniformity of the light and dark elements of the code = cell modulation (CM); (iv) damage present in the finder pattern, timing pattern, alignment pattern and the quiet zone = fixed pattern damage (FPD); (v) no uniformity between the X and Y axes of the code = axial non-uniformity (ANU); and (vi) module positioning deviation relative to the theoretical position = grid non-uniformity (GNU).

2.5. Code surface analyses by SEM

After the laser marking process, samples were cut on the reserved area using a milling cutter coupled to an OPTIMUM OPTI drill DX 15 V bench-top drilling and milling machine. For surface analyses by SEM, samples were coated with a thin gold film, and their surfaces were analyzed by SEM using a HITACHI FlexSEM 1000 model scanning electron microscope. Images were obtained at 100× and 1000× magnification in two distinct areas of the code (center and corner). Using a Bruker Quantax 80 EDS system, a sample was chemically analyzed in areas without and with laser marking.

3. Results and discussion

3.1. Quality analysis of the codes

The quality of the codes was analyzed following the ISO/IEC 29158:2020 standard [29], with the use of a microscope Verifier for this purpose, as previously mentioned. Table 3 shows different examples of DMC analyses of quality grades obtained by the microscope. These samples represent the best set of code quality classes obtained from the laser-marking parameters. The overall quality class assigned to a code corresponds to the minimum of all the features evaluated according to the parameters presented in section 2.4.

In Table 3, sample VIII, a DMC is presented with quality A (4.0) in all its features; therefore, its overall quality rating is A (4.0). In contrast, sample V, shows a DMC with an overall quality rating of F (0.0) because it has a reflectance value of 4% against a minimum requirement of 5%. It is rated F (0.0), as it does not reach the minimum required value. Even though cell modulation (CM) is rated 2.0 (C), fixed pattern damage (FPD) is rated 3.0 (B), and the remaining features are rated 4.0 (A), the overall quality grade assigned to this code is F (0.0), as it is limited to the lowest ranking of all the characteristics that have been evaluated. All codes, even those with quality F, were decodable, so a positive decodability result was obtained for all DMC.
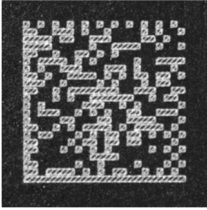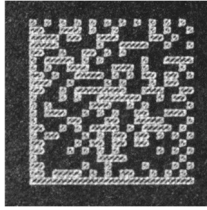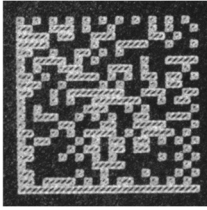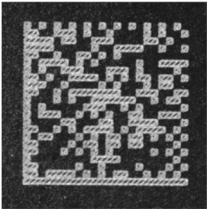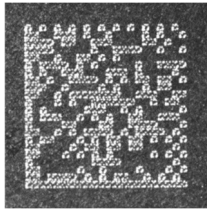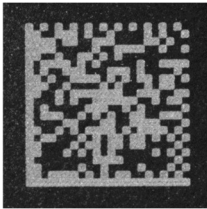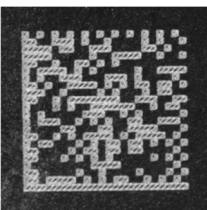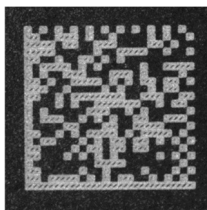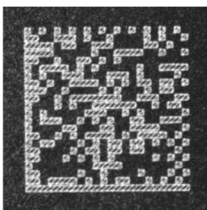
The difference between the two results is due to the choice of laser marking parameters. The marking of sample VIII was acquired using values of radiance, frequency and pass overlap higher than the nominal values indicated by the manufacturer (radiation power: 19 W, pulse frequency: 30 kHz, and pass overlap: 30%). Only the marking speed was lower than the nominal value recommended by the manufacturer (marking speed: 1000 mm/s). At lower speeds, as in the case of sample VIII, the laser interacts with the material for longer and modifies its aspect more. At higher speeds (marking speed: 3000 mm/s), as in the case of sample V, as the material is exposed for less time, it changes less and produces a lower-quality code.

Samples IV and IX were of quality B (3.0) according to the criteria of ISO/IEC 29158:2020 [29]. These samples were obtained with the same values of radiance (17 W) and pass overlap (15%) as the nominal values specified by the manufacturer, the only values modified being the pulse frequencies of 25 and 15 kHz and the marking speeds of 3000 and 2000 mm/s, respectively. It should be noted that increasing the marking speed reduces the quality of the code because the laser interacts with the material for a shorter period, and if the frequency is lower than that recommended by the manufacturer, the number of oscillations produced by the electric and magnetic fields during the one-second interval is lower, so the laser interacts less with the material.

Therefore, lower radiation power and pulse frequency and higher marking speed correspond to more faded resulting marking and therefore worse code quality. Regarding the pass overlap, it has no significant impact on the overall rating assigned to the code quality, as there are codes with low pass overlap and good ratings. However, this marking parameter combined with others allows more filling of the code, improving its appearance and robustness.

**Table 3.** Samples' optical image qualities after laser marking.

N	DMC	N	DMC	N	DMC
I	A	IV	B	VII	A
II	A	V	F	VIII	A
III	A	VI	A	IX	B

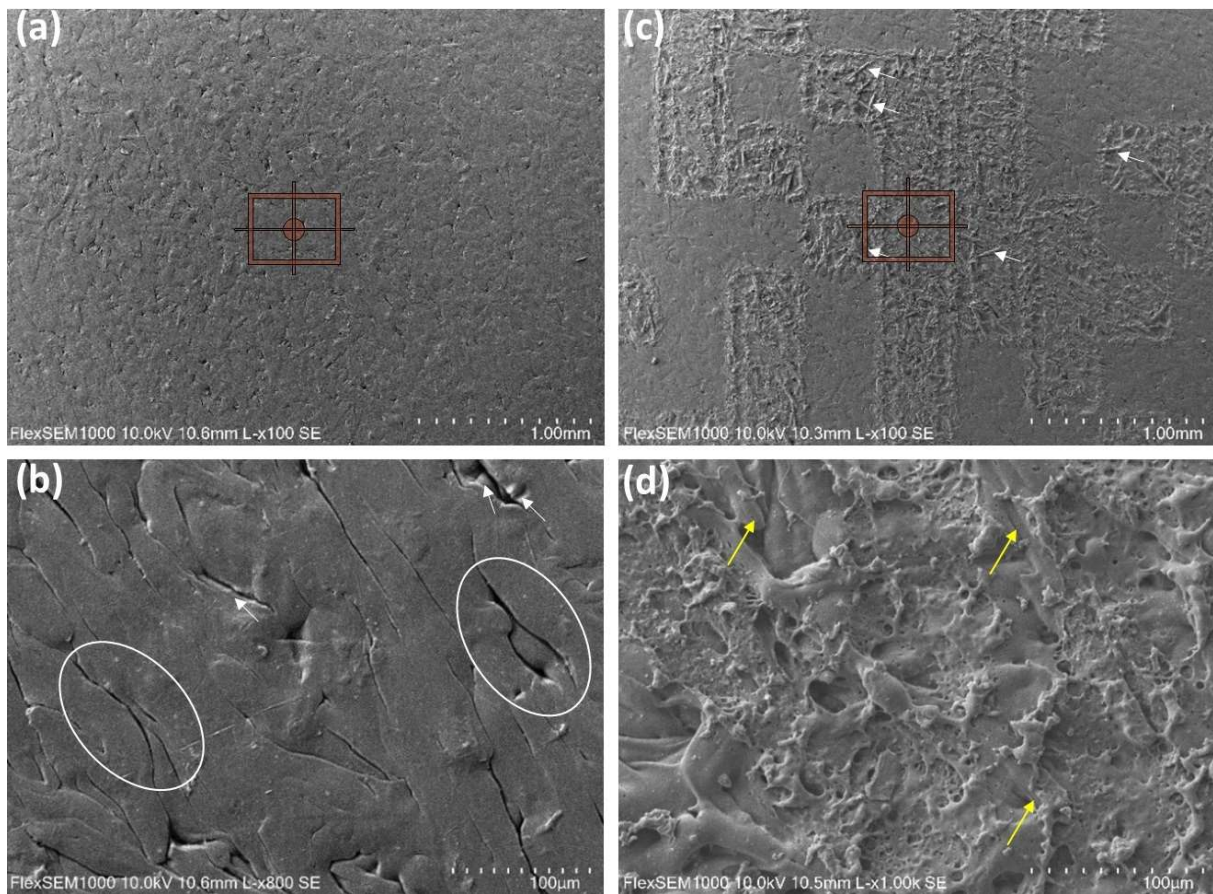### 3.2. Analysis of the marked surfaces on samples

Figure 3 presents the back housing part of the motorcycle component. Region A is the reserved area where the laser marking process is done. Regions A.1, A.2, A.3, and A.4 are the pressure points of the injection molding process. Due to the injection molding process to manufacture the back housing, the presence of stains in the reserved area surface is inherent to the process used. They usually appear in the same places and cannot be removed by the supplier, reducing the quality of the codes during the laser marking process.

Still, in Figure 3, it can be seen that the reserved area is surrounded by a white square, and four injection points are indicated by irregular spots. In the enlarged image of the reserved area, the injection defects can be seen divided into four regions (marked by numbers 1 to 4). These defects were caused by the proximity of the area to the two-injection points A.1 and A.3. Still, in the image of the reserved area (Figure 3), regions 1 and 4 have dark spots in the corner close to points A.1 and A.3. These spots are caused by the way the cavity is filled by the jet stream, known as secondary flow, in the corners of the cavity. The melt flows from the narrow gate to the wide cavity, and as the pressure increases with the injection time, the waves disappear but are still visible at the corners of the part [30], as shown in Figure 3. Region 3 has a defect known as a weld mark, represented by a dark line. This line is formed

due to the confluence of two separate streams of melting polymer with relatively low front temperatures [31]. Then, region 2 is the most suitable position for marking the DMC, because no defects are visible at this magnification.
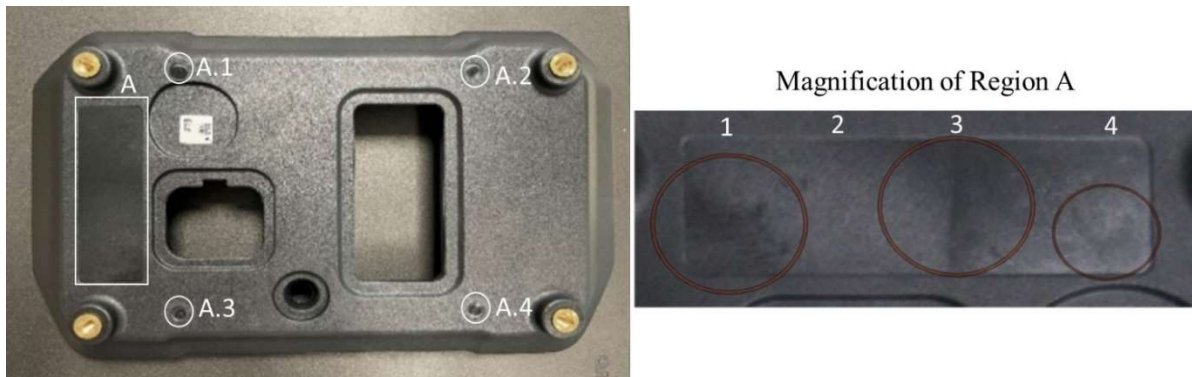
Figure 3. Reserved area surface where the DMC will be marked during production. The magnified image with the red circles shows the presence of injection marks on the surface. Region 1: secondary flow marks, region 2: no defects, region 3: weld marks, and region 4: secondary flow marks.

Figure 4. SEM analysis of PBT/GF composite surface, comparison between samples without laser marking (a, b) and with laser marking (c, d).

After the laser marking tests, the marked surfaces of several samples were analysed in detail by SEM techniques. Only DMC were selected as references. Since pass overlap is not a parameter that significantly affects the quality of the marked codes, not all samples were submitted for analysis, but only 30 with the following characteristics were submitted: (i) samples at the nominal pass overlap level but with radiation power, pulse frequency and marking speed at the minimum, nominal and maximum levels, a total of 27 samples; (ii) the samples with the best or the worst quality obtained by the microscope; and (iii) a sample without laser marking.

The first step was to analyse the material surface of a sample without laser marking (Figure 4a,b) and compare it with a sample with laser marking (Figure 4c,d). In Figure 4a, it can be seen that the unmarked sample has a more homogeneous surface than the marked sample (Figure 4c), which is uneven due to the passage of the laser beam. When the unmarked sample surface image is magnified 1000× (Figure 4b), it is possible to observe some gaps in polymeric mass promoted by pellets stretching during the injection process. These defects could be promoted by two factors that typically occur under high-speed injection molding, the mold temperature and/or the particles on filled polymer materials. According to Gim and Turng [32], during the filling and packing stages, the reinforcing fibers and particles restrict the flow of the matrix polymer material. The matrix polymer material cannot contact the mold surface sufficiently, presenting irregular whitish marks on the surface. Combined with the mold temperature, the melted polymer will cool abruptly once it contacts the cold cavity surface during filling, and its fluidity will be significantly reduced [33]. This promotes gaps in the polymeric matrix (white circles, Figure 4b) and exposes the glass fibers (yellow arrows, Figure 4d).

The sample surface after the laser marking process is presented in Figure 4c,d. It can be seen that after the code production, some glass fibers are exposed, represented by needle aspects indicated by white arrows in Figure 4c. Figure 4d is a laser marking region magnified 1000×. In that image, one can see the rough surface due to the melting of the polymeric matrix, represented by some surface aspects such as depressed holes and irregular protrusions [33]. The melting of the polymeric matrix induced by the laser action in contact with the surface causes the exposure of the short-glass fibres used as reinforcement in this composite material, indicated by the yellow arrows (Figure 4d).

3.3. Effect of different values of radiation power

To understand the influence of radiation power value on the laser marking process, samples with radiation power lower than the manufacturer's requirements (Pi = 15 W, sample I), radiation power equal to the manufacturer's requirements (Pn = 17 W, sample VII), and radiation power higher than manufacturer's requirement (Ps = 19 W, sample II) were analysed by SEM technique and compared.

Figure 5 shows the images taken at 100× and 1000× magnification, respectively, for radiation power lower, equal to and higher than the manufacturer's recommendations (Pi, Pn and Ps). At lower magnifications (Figure 5a–c) part of the DMC marking is observed. The area marked with the red square is analyzed at higher magnifications in Figure 5d–f), possibly to observe the interaction of the laser beam markings with the surface.

At lower radiation power (Pi) (Figure 5a), the difference between the marked and unmarked surface area is not very evident, as the power applied is not high enough to generate significant changes, resulting in a faded marking. At higher magnifications (Figure 5d), marks from the laser beam can be observed, but there are not many changes in the vicinity of the marked area.

When the radiation power is changed to the power level equal to that recommended by the manufacturer (Pn) (Figure 5b), the difference between the marked and unmarked surface area is clearer than when the radiation power is lower than the manufacturer's recommended level (Pi) because the applied power is higher and produces more significant changes. At higher magnification (Figure 5e), it is also possible to observe scattered marks from the laser beam in the vicinity of the marked area and micro-holes.

The radiation power was modified to a power level higher than that recommended by the manufacturer (Ps). In Figure 5c,f, the images for this power level are presented, at 100× and 1000× magnification, respectively. The radiation power applied is higher than the power recommended by the manufacturer (Pn) resulting in a more evident marking. At higher magnifications, a more laser-attacked surface has formed, indicated by the presence of flaky regions and deep holes.

Due to the differences in the thermal properties of the deformed and undeformed regions of the polymer matrix [34], the thermal energy released during the laser marking process increases the temperature, reaching the glass transition temperature for amorphous polymers and the crystallite melting temperature for semi-crystalline polymers. Molecular relaxation increases, and the melted material leads to changes in the surface topography and defects such as stress-associated dislocations [35], and blurred characters would be seen through surface lift and memory effect [36].

Many matrix dislocations were observed, evidenced by holes in areas between the fused zones (marked area, red circle) in the polymer matrix. These defects can form peaks and valleys, creating occluded areas that act as cracks [33,37].

For some polymeric matrices, some components are added to promote physical and chemical modification. In the case of acrylonitrile butadiene and styrene/organically modified montmorillonite (ABS/OMMT) composite, the laser marking process generates deep holes with irregular internal structures due to the melting, pyrolysis and carbonization of the ABS matrix at the area due to the high temperature induced by the presence of OMMT particles after laser marking process [38].

This phenomenon occurs because to obtain a good response during the laser marking, chemical components are added to the polymer matrix. These additives can absorb the laser light, convert it into thermal energy and modify the neighborhood in which they are inserted. According to the material safety data sheet of the material analyzed in this work, the Ultradur B 4406 G6 PBT-GF30 FR(17) (BASF) [28] is composed of 49% PBT, 30% GF, 1% carbon black, 5.5% antimony trioxide (Sb_2O_3), 13% halogenated compound (fire retardant), and 1.5% further additives. In this case, the PBT matrix only has a physical reaction, such as melting, that occurs during the laser marking process.
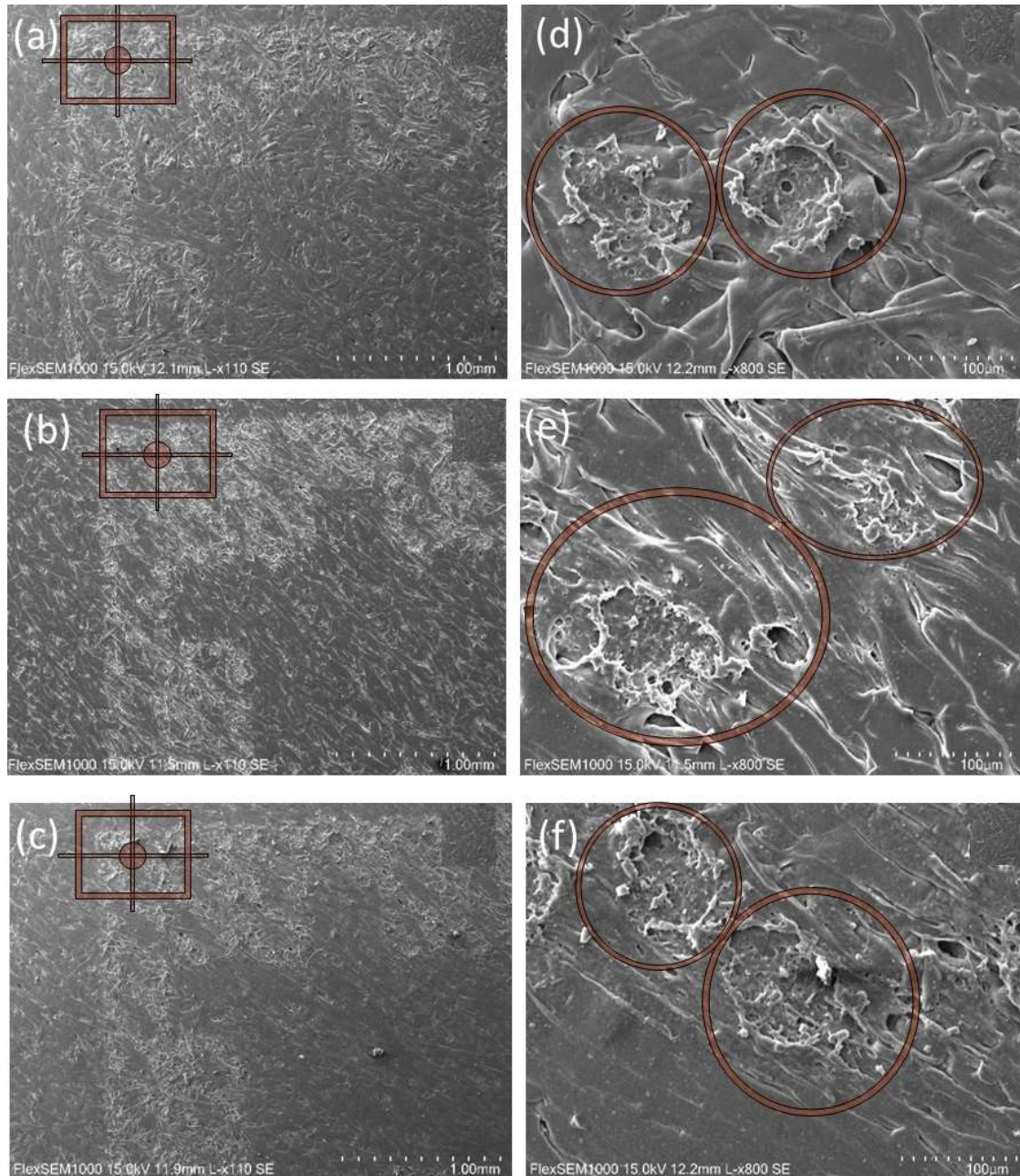
Figure 5. SEM images with (a and d) radiation power lower than the manufacturer's requirements (Pi = 15 W, sample I), (b and e) radiation power equal to the manufacturer's requirements (Pn = 17 W, sample VII), and (c and f) radiation power higher than the manufacturer's requirement (Ps = 19 W, sample II), at 100× and 1000× magnifications, respectively.

To understand the influence of pulse frequency on the laser marking surface, parameters with values lower than (Fi = 15 kHz), equal to (Fn = 25 kHz), and higher than the manufacturer's requirement (Fs = 30 kHz) were tested. Samples IX, VII and III were analyzed and compared by SEM. Figure 6 shows the images taken at 100× and 1000× magnification, respectively, with pulse frequency lower than, equal to, or higher than the manufacturer's recommendations (Fi, Fn, and Fs). At the lower, 100× magnifications (Figure 6a–c), part of the DMC marking was observed. The area marked

with the red square was analyzed at the higher, 1000× magnifications (Figure 6d–f), making it possible to observe the interaction of the laser beam markings with the surface.

Figures 6a,d show the images taken with a pulse frequency lower than that recommended by the manufacturer (Fi), at 100× and 1000× magnifications, respectively. The difference between the marked and unmarked area is not very clear, as the applied pulse frequency is not high enough to obtain a continuous marking. At the higher magnification, 1000×, it is possible to observe the laser beam marking a homogeneous surface, indicated by the presence of micro-holes and a deformed polymer matrix caused by the melting process promoted by the local heating caused by the radiant energy absorbed by the material and converted into thermal energy [27,38]. In some cases, the surface modifications that can be observed on the surfaces of polymeric materials are (1) black marking due to carbonization, (2) microvoids due to foam formation, and (3) color changes due to laser-induced thermo-chemical reactions of pigmented polymers [38]. On surfaces rich in glass fibres, the results are inferior because the temperature released by the 250 °C laser is not high enough [28] to modify the surface of the glass fibres.

If the pulse frequency is changed to a level equal to that recommended by the manufacturer (Fn), the laser marks on the sample surface (Figure 6b) are more visible compared to the pulse frequency level lower than that recommended by the manufacturer (Fi). The higher pulse frequency applied makes it possible to obtain a more continuous marking on the sample surface. In Figure 6e, it is possible to observe, at higher magnifications, the laser marks that appear deeper and more continuous compared to the previous scenario, and some exposed glass fibres can also be seen (yellow arrows).

After changing the pulse frequency to a level higher than the manufacturer's specifications (Fs), it was possible to observe a more pronounced difference between the marked and unmarked surface (Figure 6c,f). Figure 6c shows a clearer and more continuous marking compared to Figure 6b. At higher magnifications, it is possible to observe a deeper marking with larger holes (red circle, Figure 6d) and more exposed fibres (Figure 6f) than in the previous case (Figure 6e), resulting from a more sequential laser beam.

According to Man et al. [39], the amount of matrix removed depends on the total number of pulses. As the number of laser pulses was increased, the glass fibres were gradually exposed. However, as the energy density was increased, the damage to the glass fibre gradually became apparent, as shown by the thermally distorted fibres.
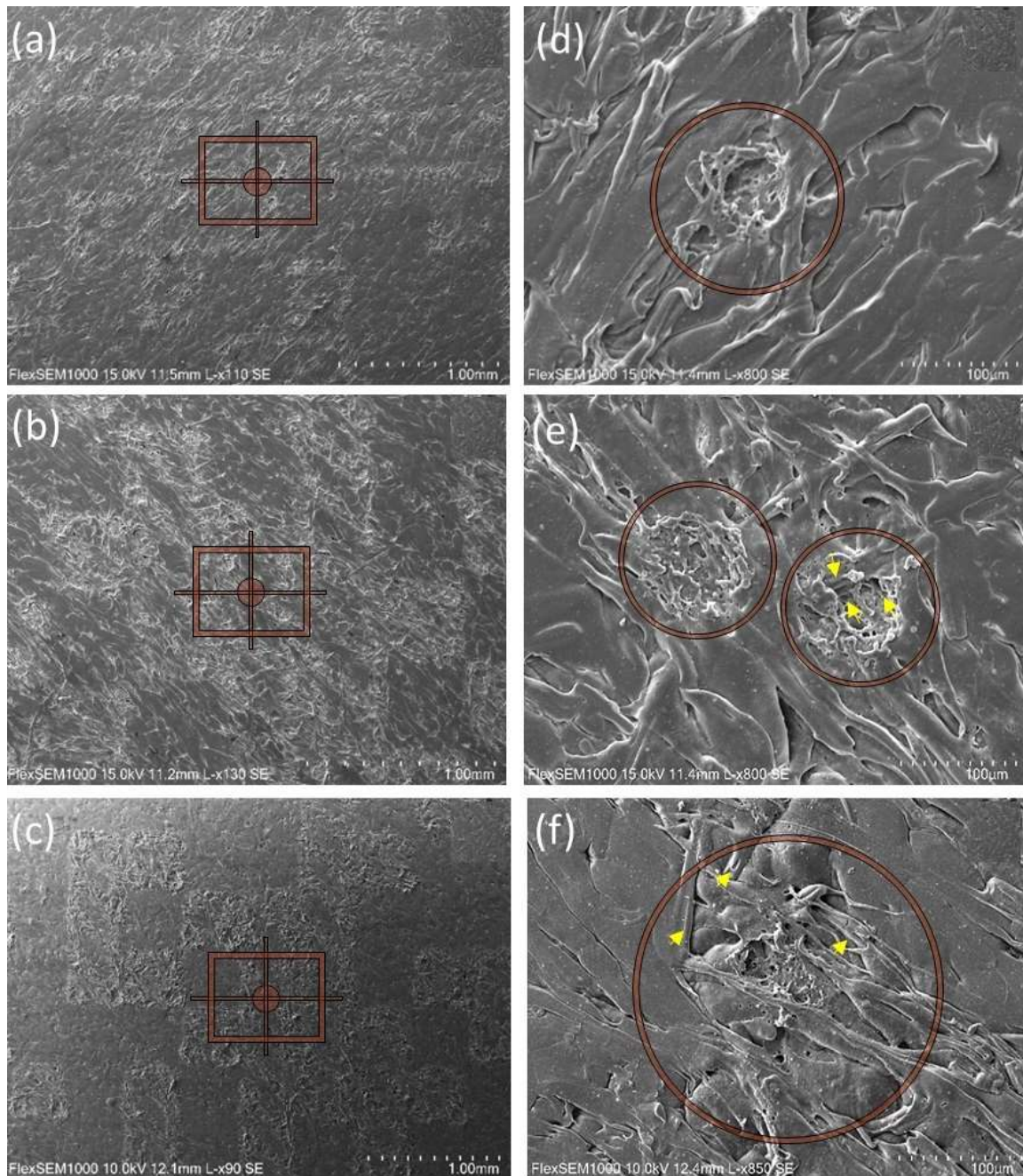
Figure 6. SEM images with (a and d) pulse frequency lower than the manufacturer's requirements (Fi = 15 kHz, sample IX), (b and e) pulse frequency equal to the manufacturer's requirements (Fn = 25 kHz, sample VII), and (c and f) pulse frequency higher than the manufacturer's requirement (Fs = 30 kHz, sample III), at 100× and 1000× magnifications, respectively.

Figure 7 shows the images obtained using the SEM technique with a marking speed lower than that recommended by the manufacturer (Vi = 1000 mm/s, sample VI), equal to that recommended by the manufacturer (Vn = 2000 mm/s, sample VII) and higher than that recommended by the manufacturer (Vs = 3000 mm/s, sample IV), at 100× and 1000× magnification, respectively.
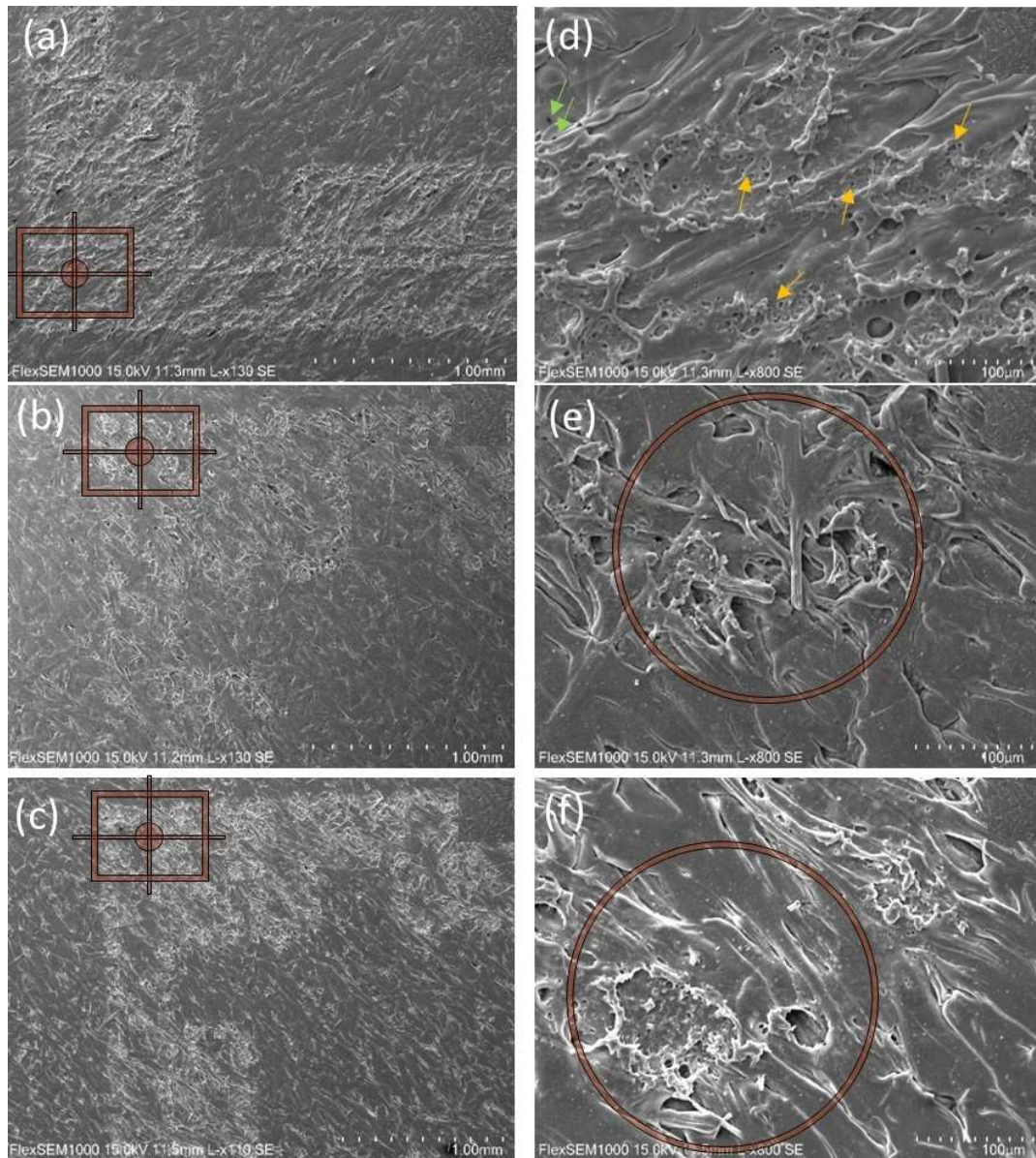
Figure 7. SEM images with (a and d) marking speed lower than the manufacturer's requirements (Vi = 1000 mm/s, sample VI), (b and e) marking speed equal to the manufacturer's requirements (Vn = 2000 mm/s, sample VII), and (c and f) marking speed higher than the manufacturer's requirement (Vs = 3000 mm/s, sample IV), at 100× and 1000× magnifications, respectively.

In Figure 7a,d, a marking speed lower than that recommended by the manufacturer (Vi) was used. The difference between the marked and unmarked surface area is quite obvious, as the selected speed is low, resulting in a longer laser interaction time with the part, causing significant surface changes. At higher magnifications, at 1000× magnification, some microvoids (yellow arrows) due to foam formation and black points (green arrows) due to polymeric matrix pyrolysis on a continuous marking surface can be observed. This phenomenon is promoted by the additives which are often dispersed in the polymer matrix. They can absorb the laser energy and locally heat the surrounding polymer chains, revealing some patterns during the laser marking process [39,40].

It is observed that after changing the marking speed to a speed level equal to that recommended by the manufacturer (Vn) (Figure 7b,e), the difference between the marked and unmarked surface area is not as clear compared to the marking speed level lower than that recommended by the manufacturer (Vi). This is because the higher the speed is, the shorter the laser interaction time is, generating less significant surface changes, presenting discontinuous surface marking, which can be observed in Figure 7e. It can be seen next to non-uniform holes formed by ablation process [41].

The image obtained from a higher marking speed than recommended by the manufacturer (Vs) is shown in Figure 7c,f. In the images obtained from samples subjected to this speed level, it is not possible to observe the difference between the marked and unmarked surface area. The marking speed is higher than the manufacturer's recommendation, resulting in a surface appearance with little change and a faded mark. At higher magnifications (Figure 7f), it is possible to observe that the material has a surface with a poor attack by the laser.

Figure 8 presents the surface of sample VIII after the laser marking process, which contains the code with the best quality of the set samples. In this sample, the difference between the marked and unmarked surface area can be observed. The surface resulting from the combination of parameters turns out to be more attacked by the laser and with continuous marking, presenting a large number of deformed regions and black points that can be observed in Figure 8b.

Comparing the surface of sample VIII (Figure 8) with sample V (Figure 9) using SEM, it can be observed that as the pulse frequency, radiation power and pass overlap are increased to levels higher than those recommended by the manufacturer, and the marking speed set for levels below the recommendation, the surface is more attacked, and the marking becomes more visible and continuous, due to greater interaction of the laser with the material.
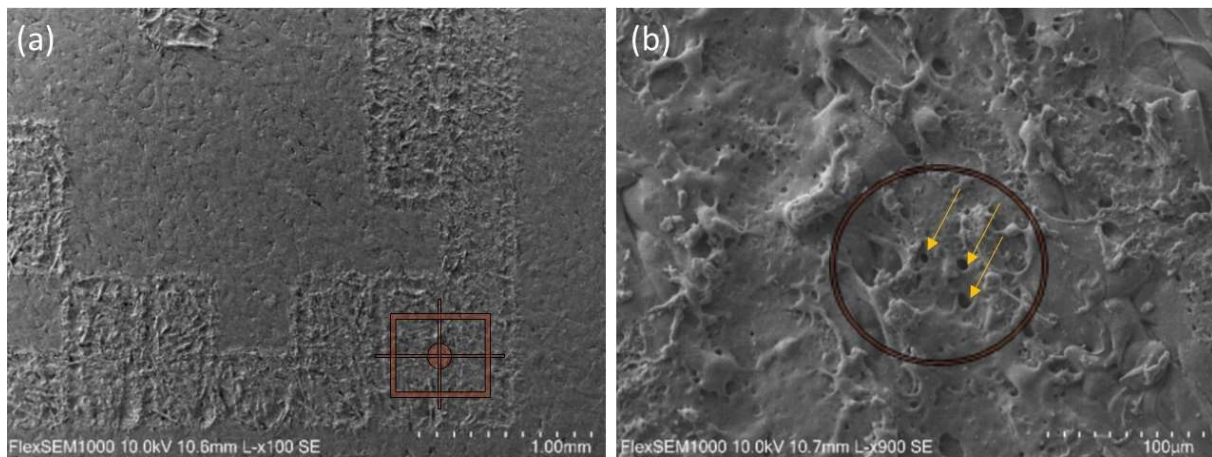
Figure 8. SEM images of sample VIII: (a) 100× magnification and (b) 1000× magnification. Laser marking parameters: radiation power: 19 W, pulse frequency: 30 kHz, pass overlap: 30%, and marking speed: 1000 mm/s.

In contrast, in Figure 9 the surface of sample V can be seen, which contains the code that has the worst quality of all sets of samples. In this sample, it is not possible to see the difference between the marked and unmarked surface area. The combination of parameters results in a surface appearance

with little change and a faded marking. In Figure 9b, at higher magnification, it can be seen that the material has an almost homogeneous surface with little deformation on the PBT matrix surface.
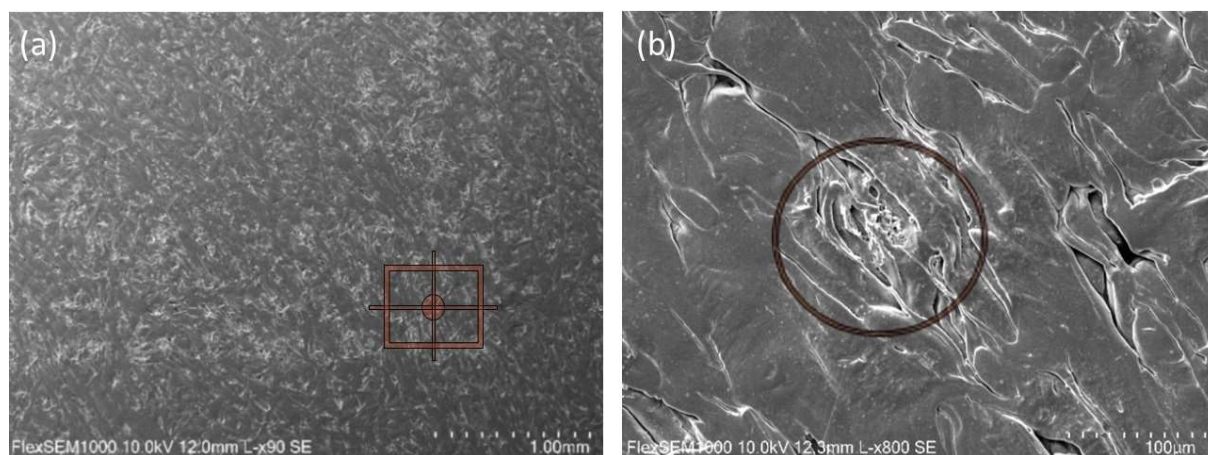
Figure 9. SEM images of sample V: (a) 100× magnification and (b) 1000× magnification. Laser marking parameters: radiation power: 15 W, pulse frequency: 15 kHz, pass overlap: 0%, and marking speed: 3000 mm/s.

## 3.4. Analysis of chemical composition after the laser marking process

Using a proprietary EDS system, sample VIII was chemically analyzed in areas without laser marking (Figure 10a) and with laser marking (Figure 10b). During EDS analysis in a polymeric material, elements such as carbon (C) and hydrogen (H) predominate. In the case of PBT, which has the chemical formula $(C_{12}H_{12}O_4)_n$, components such as carbon, hydrogen and oxygen can be detected in high quantities. The results obtained are semi-quantitative because the equipment cannot detect the chemical element H, which greatly impacts the percentages obtained. The normalized mass concentration of each chemical element present on the surface of sample VIII is shown in Figure 10.

The presence of Br and Sb components on PBT/GF composite was confirmed by EDS analysis, as shown in Figure 10. As mentioned earlier, these additives improve the laser marking process absorbing the laser energy and turning it into thermal energy, heating the vicinity and melting the polymeric matrix [39].

As mentioned by the manufacturer, carbon black is also present in the polymer matrix but was not identified separately by the EDS technique. The carbon black also improves the marking contrast. It absorbs the laser light and converts it into thermal energy, increasing the local temperature in the polymeric matrix, and helping to melt it.

It is well known that the addition of antimony compounds, such as antimony trioxide (Sb_2O_3), gives a strong synergy when used with halogen-containing compounds. Bromine is widely used as the primary flame-retardant ingredient with antimony trioxide as a synergist [40,42].

Cheng et al. [43] observed the same phenomenon in laser marking in TPU/Sb_2O_3 composite studies. In the laser marking process, Sb_2O_3 particles absorb the laser and convert it into thermal energy, and the crystal structure of Sb_2O_3 does not change according to XRD analysis. The EDS analysis revealed that there is no difference in chemical composition between these two areas, indicating that the laser parameters used do not cause chemical changes on the surface.
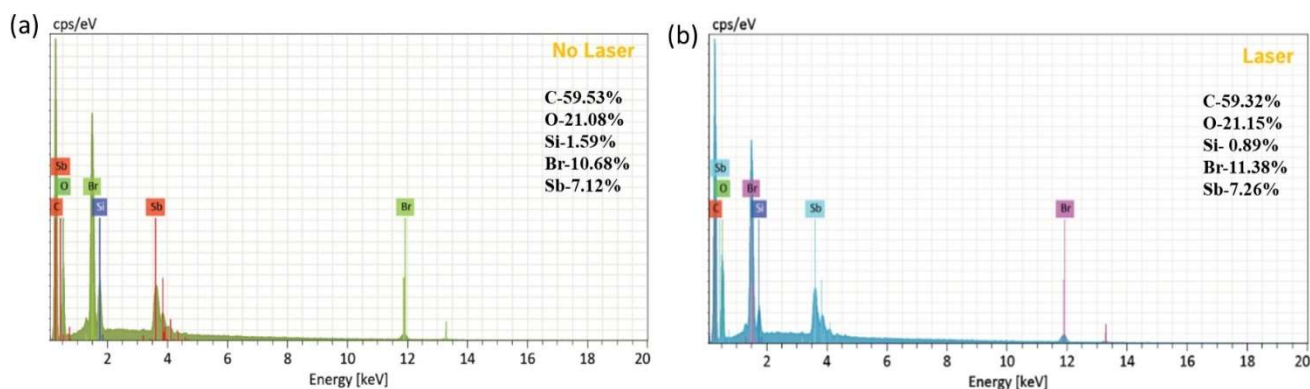
Figure 10. Chemical analysis of sample VIII, normalized mass concentration of each chemical element (%): (a) area without laser marking and (b) area with laser marking.

4. Conclusions

A systematic study was carried out to improve the quality of DMC on a PBT/GF composite surface obtained by laser marking. The samples were subjected to laser parameters lower than, equal to, and higher than the manufacturer's requirements, and the sample surface was microscopically analyzed using a microscope Verifier and SEM.

All marked codes were optically analyzed using a microscope, and the ISO/IEC 29158:2020 classification was accurately obtained. It was confirmed that lower radiation power and pulse frequency and higher marking speed corresponded to fainter resulting marking and, therefore, poorer code quality. Pass overlap does not have a significant effect on the overall code quality score, as there are codes with low pass overlap and good scores. However, this marking parameter allows the code to be more complete, improving its appearance and robustness.

The same surface aspects of the samples observed using optical analysis with the Verifier were confirmed using SEM, which made it possible to analyze the marked surfaces of several samples in detail and study the effect of the parameters on the surface changes.

Radiation power lower than that recommended by the manufacturer is not sufficient to produce obvious changes between the marked and unmarked surface, resulting in blurred markings and deep holes. Increasing the power to levels equal to or greater than those recommended by the manufacturer, while maintaining the pulse frequency, marking speed and passage overlap at levels recommended by the manufacturer, will make the marking more visible. It is possible to observe the presence of flaky areas, and deep holes can be observed. The defects observed are caused by the thermal effects of the laser improved by the additives, carbon black and Sb_2O_3, which have melted the material and caused changes in the surface topography.

A pulse frequency lower than the manufacturer's recommended is insufficient to produce obvious changes between marked and unmarked areas, resulting in intermittent and therefore discontinuous marking. Increasing the pulse frequency to levels equal to or greater than those recommended by the manufacturer, while maintaining the radiant power, marking speed and passage overlap at levels recommended by the manufacturer, will cause the surface to be more attacked and the marking to become more visible and continuous because of a more sequential laser beam and therefore greater interaction between the laser and the part.

A marking speed higher than the manufacturer's recommended speed is not sufficient to produce clear changes between the marked and unmarked areas, resulting in a blurred marking. Reducing the marking speed to levels equal to or less than those recommended by the manufacturer, while maintaining the radiant power, pulse frequency and pass overlap at levels recommended by the manufacturer, will make the marking more visible and continuous. This is because the lower the speed is, the more the laser interacts with the part, causing significant surface changes. It was concluded that the lower radiation power levels, lower pulse frequencies and higher marking speeds resulted in barely visible marking. The surface aspects were represented by the polymeric matrix melting and some glass fibers being visible but with the polymeric matrix adhered to the fiber surface.

It was concluded that higher pulse frequencies and lower marking speeds result in a greater surface attack by the laser and a more continuous marking, as the greater the interaction of the laser with the part is, the greater the surface changes. The surface aspects, in these cases, present flaky regions and deep holes.

The laser only affects the physical properties during the marking process, melting the PBT polymer matrix as the code is recorded. EDS analysis showed that the laser marking process did not significantly affect the chemical composition of the samples.

Use of AI tools declaration

The authors declare they have not used artificial intelligence (AI) tools in the creation of this article.

Acknowledgments

Conflict of interest

The authors declare no conflict of interest.

References

1. Marin-Garcia JA, Pardo del Val M, Bonavía Martín T (2008) Longitudinal study of the results of continuous improvement in an industrial company. *Team Perform Manag* 14: 56–69. https://doi.org/10.1108/13527590810860203
2. Grütter AW, Field JM, Faull NHB (2002) Work team performance over time: Three case studies of South African manufacturers. *J Oper Manag* 20: 641–657. https://doi.org/10.1016/S0272-6963(02)00031-1
3. Bosch (2021) *Good Service Practices Manual*. BOSCH Internal release, Braga, Portugal.
4. Barad M (2014) Design of experiments (DoE)—A valuable multi-purpose methodology. *Appl Math* 5: 2120–2129. https://doi.org/10.4236/am.2014.514206

5. Loh SH, The PC, Sim JJ, et al. (2023) Decoding dot peen data matrix code with deep learning capability for product traceability. *AMS* 7: 38–48. Available from: http://arqiipubl.com/ojs/index.php/AMS_Journal/article/view/385.

6. Li C, Lu C, Li J (2018) Research on the quality of laser marked data matrix symbols. *Key Eng Mater* 764: 219–224. https://doi.org/10.1088/1757-899X/380/1/012023

7. Sobotova L, Demec P (2015) Laser marking of metal materials. *MM Sci J* 12: 808–812. https://doi.org/10.17973/MMSJ.2015_12_201410

8. Javale V, Nair VA (2013) Review on laser marking by Nd-Yag laser and fiber laser. *Int J Sci Res Dev* 1: 1995–1997. Available from: https://ijsrd.com/Article.php?manuscript=IJSRDV1I9075.

9. Trotec Laser (2019) *Laser handbook: A comprehensive guide to industrial laser applications*, Austria: Trotec Laser.

10. Qi J, Wang K, Zhu Y (2003) A study on the laser marking process of stainless steel. *J Mater Process Technol* 139: 273–276. https://doi.org/10.1016/S0924-0136(03)00234-6

11. Jangsombatsiri W, Porter JD (2007) Laser direct-part marking of data matrix symbols on carbon steel substrates. *J Manuf Sci E-T ASME* 129: 583–591. https://doi.org/10.1115/1.2716704

12. Zelenska KS, Zelensky SE, Poperenko LV, et al. (2016) Thermal mechanisms of laser marking in transparent polymers with light-absorbing microparticles. *Opt Laser Technol* 76: 96–100. https://doi.org/10.1016/j.optlastec.2015.07.011

13. Czyzewski P, Sykutera D, Rojewski M (2022) The impact of selected laser-marking parameters and surface conditions on white polypropylene moldings. *Polymer* 14: 1879. https://doi.org/10.3390/polym14091879

14. Lu G, Wu Y, Zhang Y, et al. (2020) Surface laser-marking and mechanical properties of acrylonitrile-butadiene-styrene copolymer composites with organically modified montmorillonite. *ACS Omega* 5: 19255−19267. https://dx.doi.org/10.1021/acsomega.0c02803

15. Narica P, Fedotovs J (2019) Marking of a small-sized QR code on a plastic surface. 19th International Conference on Reliability and Statistics in Transportation and Communication, Riga, Latvia Springer, 16–19. https://link.springer.com/chapter/10.1007/978-3-030-44610-9_41

16. Li WH (2021) Preparation of laser markable polyamide compounds. 2nd International Conference on Graphene and Novel Nanomaterials (GNN), 1765: 1–5. https://doi.org/10.1088/1742-6596/1765/1/012003

17. Chen MF, Hsiao WT, Huang WL, et al. (2009) Laser coding on the eggshell using pulsed laser marking system. *J Mater Process Technol* 209: 737–744. https://doi.org/10.1016/j.jmatprotec.2008.02.075

18. Cheng J, Zhou J, Zhang C, et al. (2019) Enhanced laser marking of polypropylene induced by "core-shell" ATO@PI laser-sensitive composite. *Polym Degrad Stabil* 167: 77–85. https://doi.org/10.1016/j.polymdegradstab.2019.06.022

19. Yang J, Xiang M, Zhu Y, et al. (2023) Influences of carbon nanotubes/polycarbonate composite on enhanced local laser marking properties of polypropylene. *Polym Bull* 80: 1321–1333. https://doi.org/10.1007/s00289-022-04123-3

20. Zhong W, Cao Z, Qiu P, et al. (2015) Laser-marking mechanism of thermoplastic polyurethane/Bi$_2$O$_3$ composites. *ACS Appl Mater Interface* 7: 24142−24149. https://doi.org/10.1021/acsami.5b07406

21. Cao Z, Hu Y, Lu Y, et al. (2017) Laser-induced blackening on surfaces of thermoplastic polyurethane/BiOCl composites. *Polym Degrad Stabil* 141: 33–40. http://dx.doi.org/10.1016/j.polymdegradstab.2017.05.004

22. Ng TW, Yeo SC (2000) Aesthetic laser marking assessment. *Opt Laser Technol* 32: 187–191. https://doi.org/10.1016/S0030-3992(00)00040-2

23. Ng TW, Yeo SC (2001) Aesthetic laser marking assessment using luminance ratios. *Opt Laser Eng* 35: 177–186. https://doi.org/10.1016/S0143-8166(01)00005-7

24. Arai S, Tsunoda S, Yamaguchi A, et al. (2019) Effect of anisotropy in the build direction and laser-scanning conditions on characterization of short-glass-fiber-reinforced PBT for laser sintering. *Opt Laser Technol* 113: 345–356. https://doi.org/10.1016/j.optlastec.2019.01.012

25. Greiner S, Wudy K, Lanzl L, et al. (2017) Selective laser sintering of polymer blends: Bulk properties and process behaviour. *Polym Test* 64: 136–144. https://doi.org/10.1016/j.polymertesting.2017.09.039

26. Silva LRR, Marques EAS, Carbas RJC, et al. (2002) Study of the optical, thermal, morphological and mechanical characteristics of a laser weldable fibre reinforced polymer. *Polym Compos* 43: 4038–4055. https://doi.org/10.1002/pc.26677

27. Ng TW, Yeo SC (2000) Aesthetic laser marking assessment using spectrophotometers. *J Mater Process Technol* 104: 280–283. https://doi.org/10.1016/S0924-0136(00)00548-3

28. BASF (2023) Product Data Sheet Ultradur B 4406 G6 05/2023 PBT-GF30 FR(17). Available from: https://www.basf.com/cn/documents/en/chinaplas/Ultradur_brochure.pdf.

29. ISO/IEC 29158 (2020) Information technology—Automatic identification and data capture techniques-Direct Part Mark (DPM) Quality Guideline.

30. Bociga E, Jaruga T (2007) Experimental investigation of polymer flow in injection mould. *Arch Mater Sci Eng* 28: 165–172.

31. Wang G, Zhao G, Wang X (2013) Effects of cavity surface temperature on reinforced plastic part surface appearance in rapid heat cycle moulding. *Mater Design* 44: 509–520. https://doi.org/10.1016/j.matdes.2012.08.039

32. Gim J, Turng LS (2022) A review of current advancements in high surface quality injection moulding: Measurement, influencing factors, prediction, and control. *Polym Test* 115: 107718. https://doi.org/10.1016/j.polymertesting.2022.107718

33. Uysal S, Mercan M, Uzun L (2020) Serial number restoration on polymer surfaces: A survey of recent literature. *Forensic Chem* 20: 100267. https://doi.org/10.1016/j.forc.2020.100267

34. Katterwe H (1994) The recovery of erased numbers in polymers. *J Forensic Sci Soc* 34: 11–16. https://doi.org/10.1016/S0015-7368(94)72876-0

35. Young RJ, Lovell PA (2011) *Introduction to Polymers*, 3 Eds., Boca Raton: CRC Press. https://doi.org/10.1201/9781439894156

36. Aly AA (2015) Heat treatment of polymers: A review. *Int J Mater Chem Phys* 1: 132–140. https://api.semanticscholar.org/CorpusID:53342231

37. Pieretti EF, Costa I (2013) Surface characterization of ASTM F139 stainless steel marked by laser and mechanical techniques. *Electrochim Acta* 114: 838–843. https://doi.org/10.1016/j.electacta.2013.05.101

38. Lu G, Wu Y, Zhang Y, et al. (2020) Surface laser-marking and mechanical properties of acrylonitrile butadiene-styrene copolymer composites with organically modified montmorillonite. *ACS Omega* 5: 19255−19267. https://doi.org/10.1021/acsomega.0c02803

39. Man HC, Li M, Yue TM (1998) Surface treatment of thermoplastic composites with an excimer laser. *Int J Adhes Adhes* 18: 151–157. https://doi.org/10.1016/S0143-7496(97)00044-4

40. Cao Z, Hu Y, Yu Q, et al (2017) Facile fabrication, structures, and properties of laser-marked polyacrylamide/Bi_2O_3 hydrogels. *Adv Eng Mater* 19: 1600826. https://doi.org/10.1002/adem.201600826

41. Obilor AF, Pacella M, Wilson A, et al. (2022) Micro-texturing of polymer surfaces using lasers: A review. *Int J Adv Manuf Technol* 120: 103–135. https://doi.org/10.1007/s00170-022-08731-1

42. Margolis JM (2006) *Engineering Plastic Handbook*, 1 Ed., New York: McGraw-Hill Professional. https://doi.org/10.1036/0071457674

43. Cheng J, Li H, Zhou J, et al. (2018) Influences of diantimony trioxide on laser-marking properties of thermoplastic polyurethane. *Polym Degrad Stabil* 154: 149–156. https://doi.org/10.1016/j.polymdegradstab.2018.05.031